10.1071/CH08563_AC

Australian Journal of Chemistry, 2009, 62(12), 1675–1683

ACCESSORY PUBLICATION

Synthesis and Structure of Novel Ru^{II}-N≡C-Me Complexes and their Activity Towards Nitrile Hydrolysis: An Examination of Ligand Effects.

Joaquim Mola,[a,‡] *David Pujol,*[a,‡] *Montserrat Rodríguez,*[a,‡] *Isabel Romero,*[*,a,‡] *Xavier Sala ,*[b] *Néstor Katz*[≠,c] *Teodor Parella,*[d,┼] *Jordi Benet-Buchholz,*[b] *Xavier Fontrodona,*[a,┼] *and Antoni Llobet.*[*,b,d,‡]

[a] *Departament de Química and Serveis Tècnics de Recerca (STR), Universitat de Girona, Campus de Montilivi, E-17071 Girona, Spain.* [b] *Institute of Chemical Research of Catalonia (ICIQ), Av. Països Catalans 16, E-43007 Tarragona, Spain,* [c] *Instituto de Química Física, Facultad de Bioquímica, Química y Farmacia, Universidad Nacional de Tucumán Ayacucho 491, (T4000INI) San Miguel de Tucumán, Argentina,*[d] *Departament de Química and Servei de RMN Universitat Autònoma de Barcelona, Cerdanyola del Vallès, E-08193 Barcelona, Spain.*

Electronic mail: ***marisa.romero@udg.es***, ***allobet@iciq.es***.

‡ Departament de Química

┼ Serveis Tècnics de Recerca

Table S1. Selected bond lengths and angles for complexes **4**, **5**, and **6**.

bond/angle	**4**	bond/angle	**5**	bond/angle	**6**
Ru(1)-N(1)	2,207(10)	Ru(1)-N(1)	2,120(4)	Ru(1)-N(1)	2,129(2)
Ru(1)-N(2)	2,019(9)	Ru(1)-N(2)	2,167(4)	Ru(1)-N(2)	2,183(2)
Ru(1)-N(3)	2,162(14)	Ru(1)-N(3)	2,120(4)	Ru(1)-N(3)	2,156(2)
Ru(1)-N(4)	1,952(10)	Ru(1)-N(4)	2,020(4)	Ru(1)-P(1)	2,2961(7)
Ru(1)-N(5)	1,984(16)	Ru(1)-P(1)	2,3134(15)	Ru(1)-P(2)	2,3207(7)
Ru(1)-N(6)	2,185(9)	Ru(1)-P(2)	2,2961(13)	Ru(1)-O(1)	2,107(2)
N(6)-C(26)	1.162(12)	N(4)-C(42)	1.123(6)		
N(1)-Ru(1)-N(2)	78,4(8)	N(1)-Ru(1)-N(2)	80,21(14)	N(1)-Ru(1)-N(2)	79,83(8)
N(3)-Ru(1)-N(2)	85,4(4)	N(3)-Ru(1)-N(2)	80,90(15)	N(3)-Ru(1)-N(2)	80,23(8)
N(6)-Ru(1)-N(1)	96,3(3)	N(4)-Ru(1)-N(1)	92,38(15)	O(1)-Ru(1)-N(1)	86,76(8)
N(6)-Ru(1)-N(2)	174,6(5)	N(4)-Ru(1)-N(2)	171,29(15)	O(1)-Ru(1)-N(2)	161,94(8)
N(6)-Ru(1)-N(3)	90,9(5)	N(4)-Ru(1)-N(3)	93,30(16)	O(1)-Ru(1)-N(3)	85,56(8)
N(1)-Ru(1)-N(4)	98,0(4)	N(1)-Ru(1)-P(1)	99,38(12)	N(1)-Ru(1)-P(1)	95,81(6)
N(2)-Ru(1)-N(4)	97,1(4)	N(2)-Ru(1)-P(1)	100,58(11)	N(2)-Ru(1)-P(1)	96,46(6)
N(3)-Ru(1)-N(4)	177,5(5)	N(3)-Ru(1)-P(1)	177,96(12)	N(3)-Ru(1)-P(1)	174,83(6)
N(6)-Ru(1)-N(4)	86,7(4)	N(4)-Ru(1)-P(1)	85,06(13)	O(1)-Ru(1)-P(1)	96,87(6)
N(5)-Ru(1)-N(4)	77,8(5)	P(2)-Ru(1)-P(1)	84,09(5)	P(2)-Ru(1)-P(1)	83,25(3)
N(1)-Ru(1)-N(5)	175,8(7)	N(1)-Ru(1)-P(2)	176,05(12)	N(1)-Ru(1)-P(2)	178,81(6)
N(2)-Ru(1)-N(5)	101,8(5)	N(2)-Ru(1)-P(2)	97,35(10)	N(2)-Ru(1)-P(2)	101,00(6)
N(3)-Ru(1)-N(5)	101,8(5)	N(3)-Ru(1)-P(2)	97,13(11)	N(3)-Ru(1)-P(2)	101,23(7)
N(6)-Ru(1)-N(5)	82,7(5)	N(4)-Ru(1)-P(2)	89,79(12)	O(1)-Ru(1)-P(2)	92,62(6)

Figure captions for supplementary information

Figure S1. NMR (500 MHz, C_2D_6O, 25 ºC) spectra for complex **4**: a) ^1H, b) COSY, c) HSQC ^1H-^{13}C, d) NOESY, e) ^1H-^{13}C HMBC, f) ^1H-^{15}N HMBC.

Figure S2. NMR (500 MHz, C_2D_6O, 25ºC) spectra for complex **5**: a) ^1H, b) COSY, c) HSQC ^1H-^{13}C, d) NOESY, e) ^1H-^{13}C HMBC, f) ^{31}P (101.26 MHz).

Figure S3. ^1H-NMR (200 MHz, C_2D_6O, 25ºC) spectra for complex **6**.

Figure S4. CV for: a) **4**, registered in CH_3CN + 0.1M TBAH, b) **5**, registered in CH_3CN + 0.1M TBAH, c) **5'**, registered in CH_2Cl_2 + 0.1M TBAH.

Figure S5. UV-visible spectrum of $[Ru(NO_3)(bpea)(dppe)]^+$, **6** registered in CH_2Cl_2, at room temperature.

Figure S6. a) UV-visible spectrum of $[Ru(OH)(bpea)(bpy)]^+$, and $[Ru(bpea)(bpy)(H_2O)]^{2+}$ registered after the addition of a drop of concentrated HCl.

Figure S7. a) Spectra obtained in aqueous basic solutions of: a) $[Ru(bpea)(dppe)(CH_3CN)]^{2+}$, **5**, at different times (*[Ru]* = 5 x 10^{-5} M*; pH* = 13; *I* = 0.1 M; *T* = 25 °C). The inset shows plots of λ= 332 nm vs. time during nitrile hydrolysis and b) Spectra obtained in aqueous basic solutions of: a) [Ru (phen)(MeCN)([9]aneS_3)]$^{2+}$, **7**, at different times (*[Ru]* = 5 x 10^{-5} M*; pH* = 13; *I* = 0.1 M; *T* = 25 °C). The inset shows plots of λ= 437 nm vs. time during nitrile hydrolysis.

Figure S8. Eyring's plot for the basic hydrolysis of CH_3CN in a) **4** b) **5** and c) **7**.

Figure S9. Dependece of the hydrolysis rate constants k_{obs} with $[OH^-]$: a) for **4** at 25ºC b) for **5** at 35ºC.

Figure S10. Schematic view of a) $Ru(bpea)(bpy)(CH_3CN)]^{2+}$, **4**, b) $Ru(bpea)(dppe)(CH_3CN)]^{2+}$, **5**, and c) $Ru(NO_3)(bpea)(dppe)]^+$, **6**, and their corresponding axial angles values. H··O hydrogen bonding distance involving the nitrate ligand is indicated in the case of complex **6**.

Figure S1.

a)

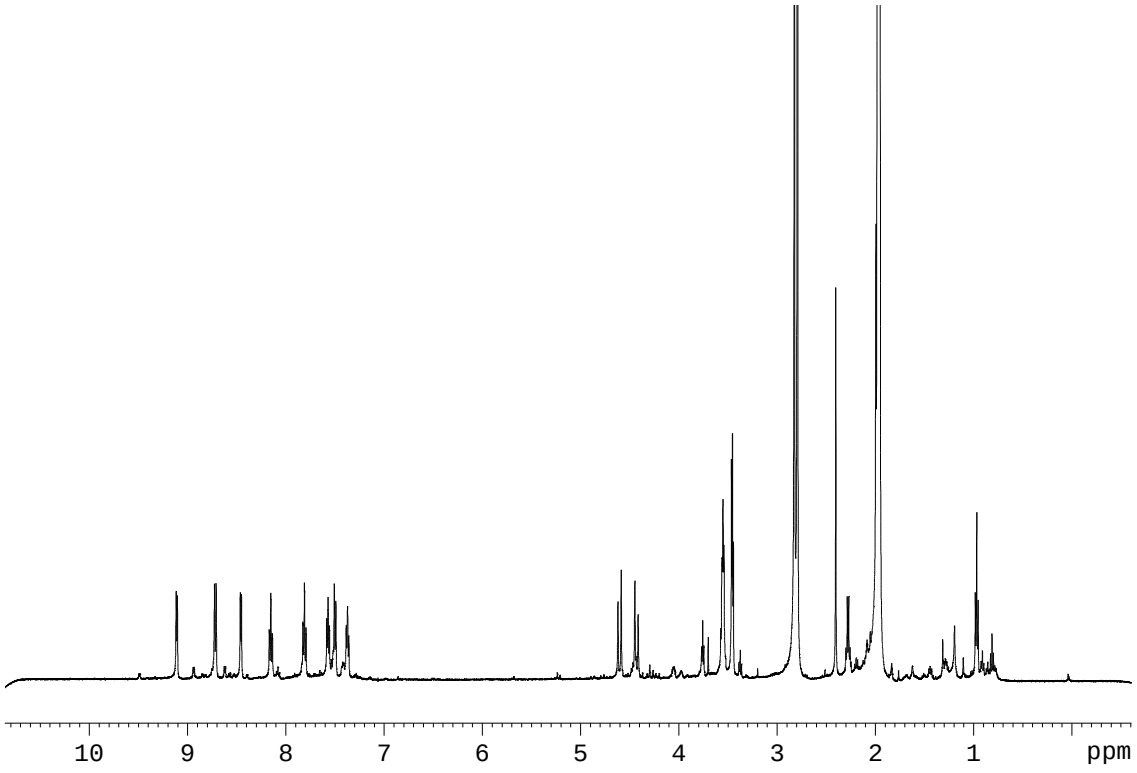

b)

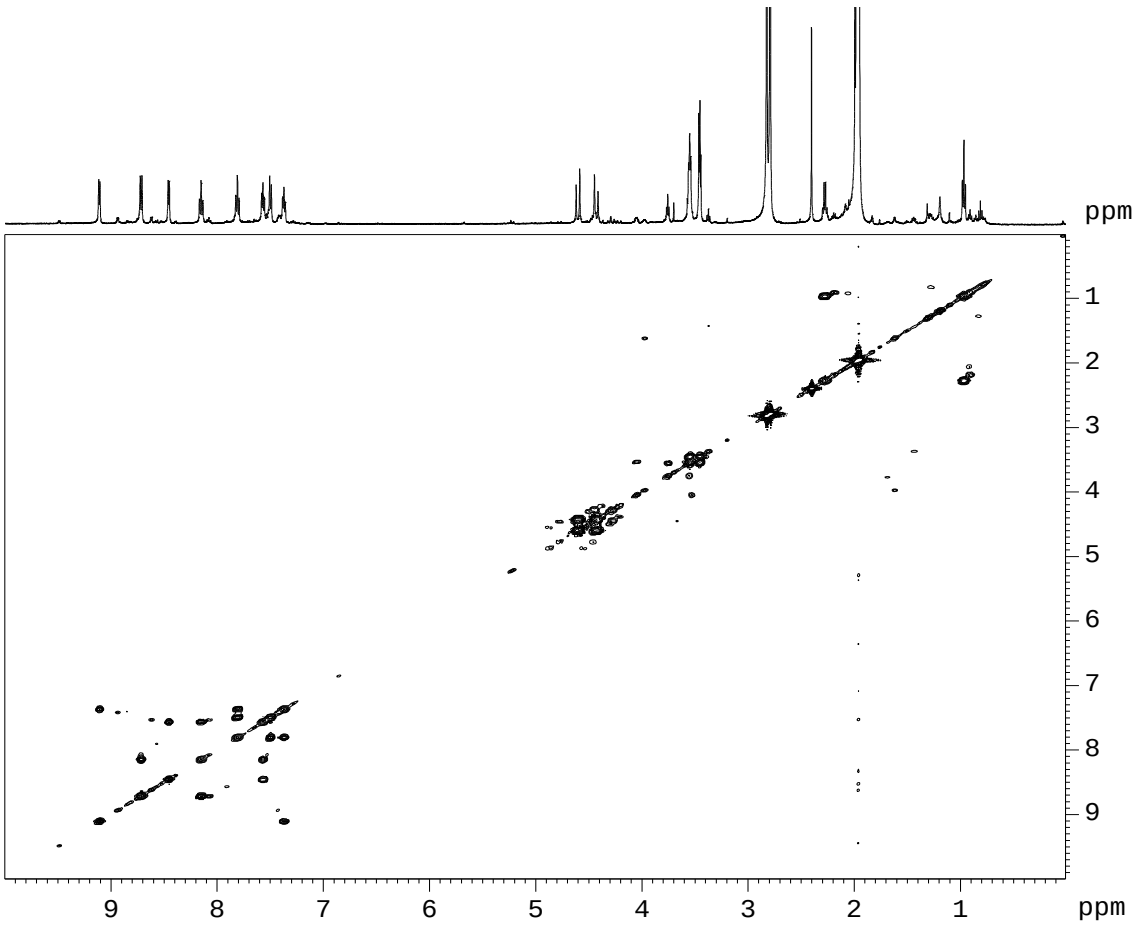

c)

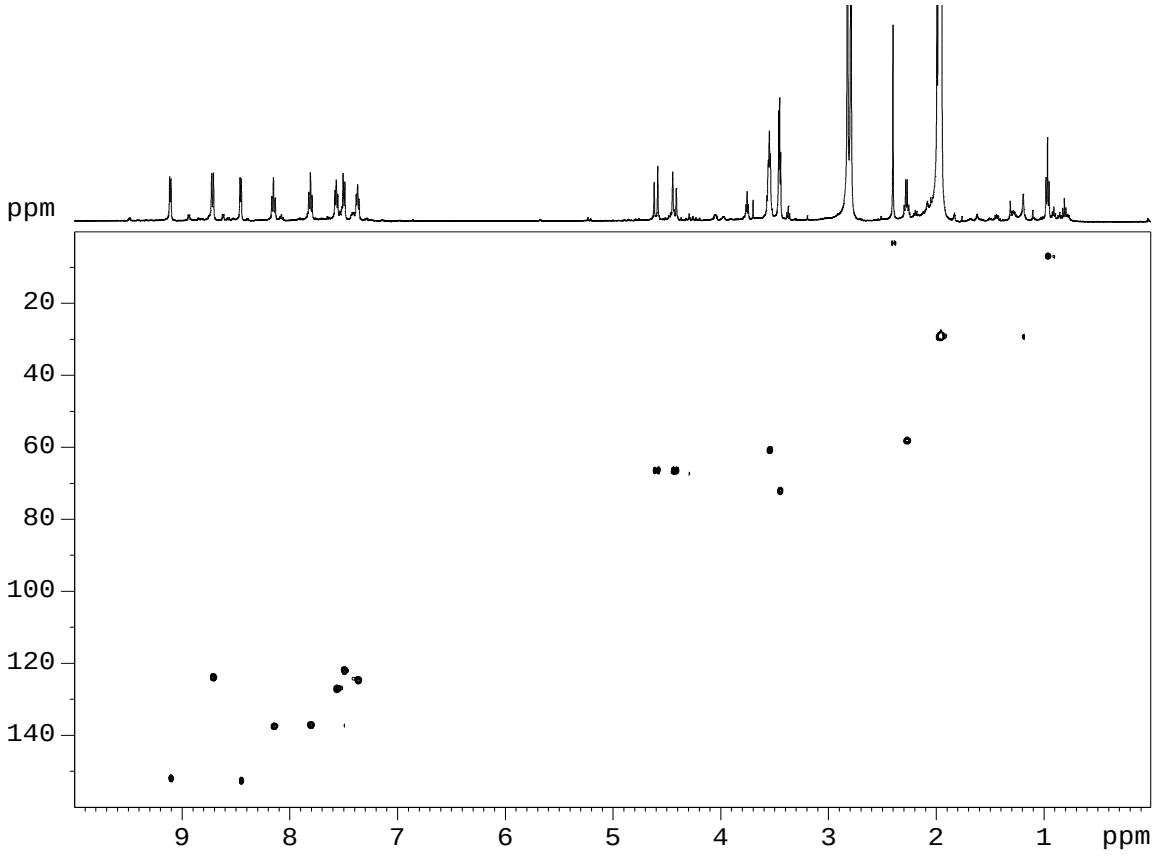
ppm
20
40
60
80
100
120
140
9
8
7
6
5
4
3
2
1
ppm

d)

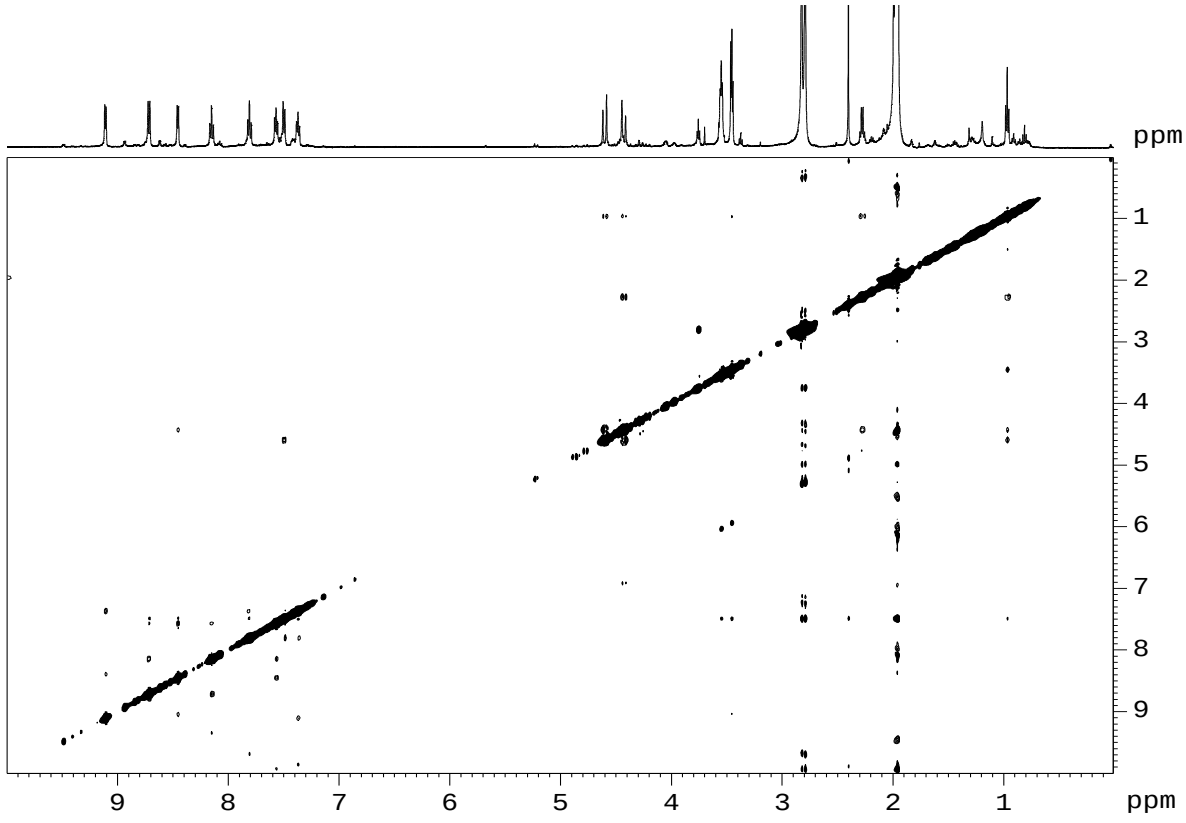
ppm
1
2
3
4
5
6
7
8
9
9
8
7
6
5
4
3
2
1
ppm

e)

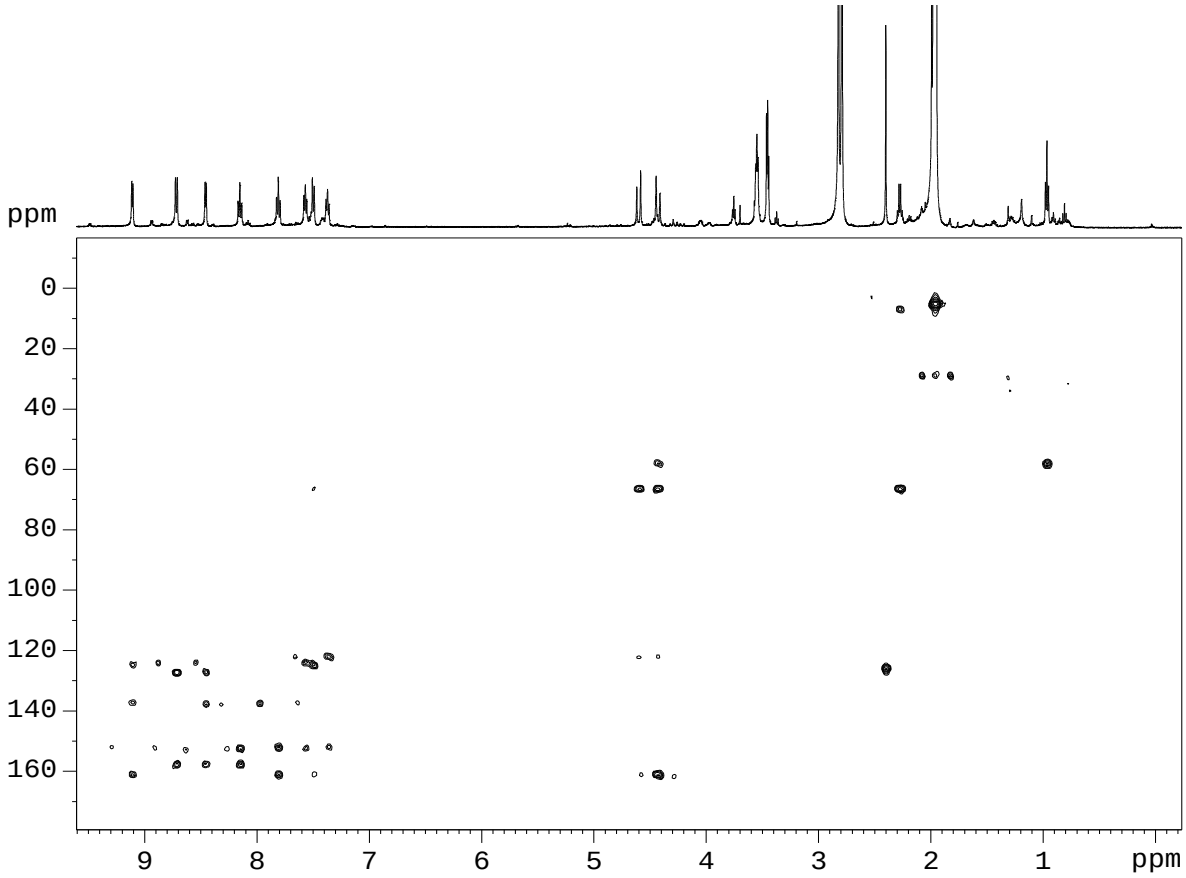
ppm
0
20
40
60
80
100
120
140
160
9
8
7
6
5
4
3
2
1
ppm

f)

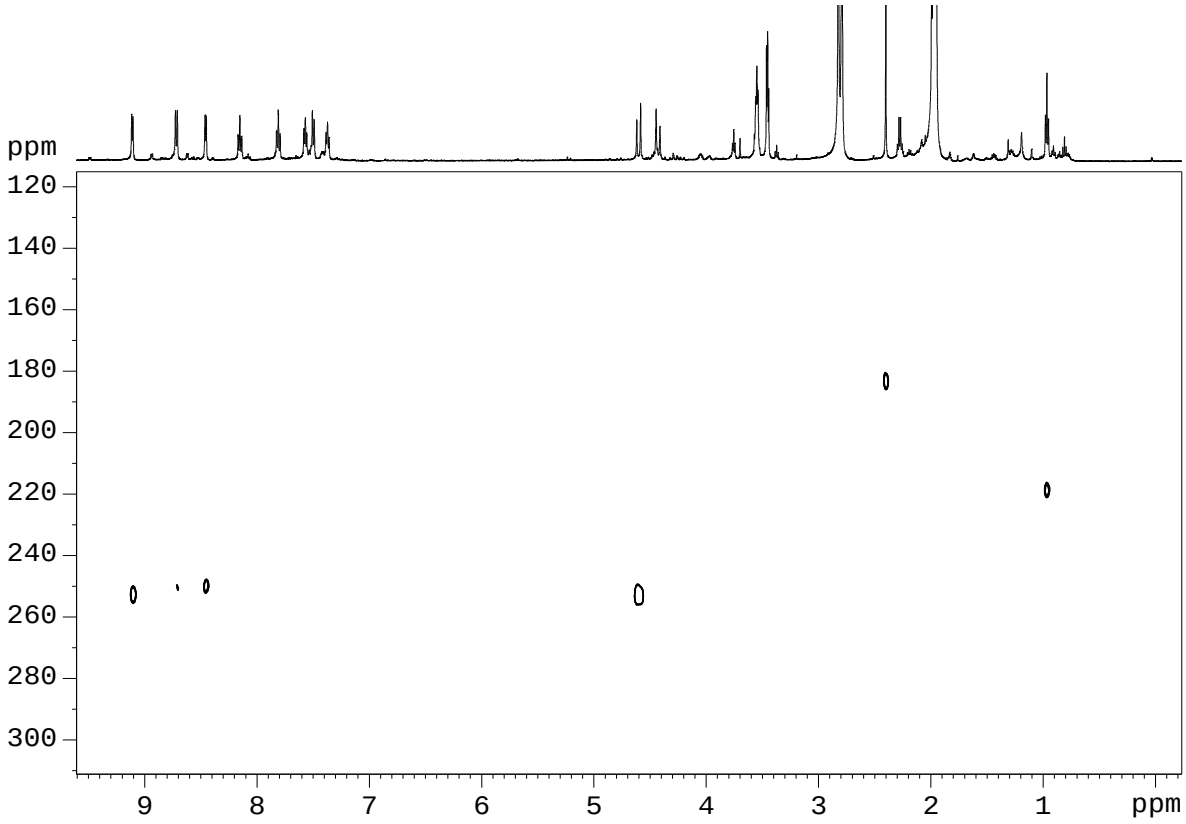
ppm
120
140
160
180
200
220
240
260
280
300
9
8
7
6
5
4
3
2
1
ppm

Figure S2.

a)

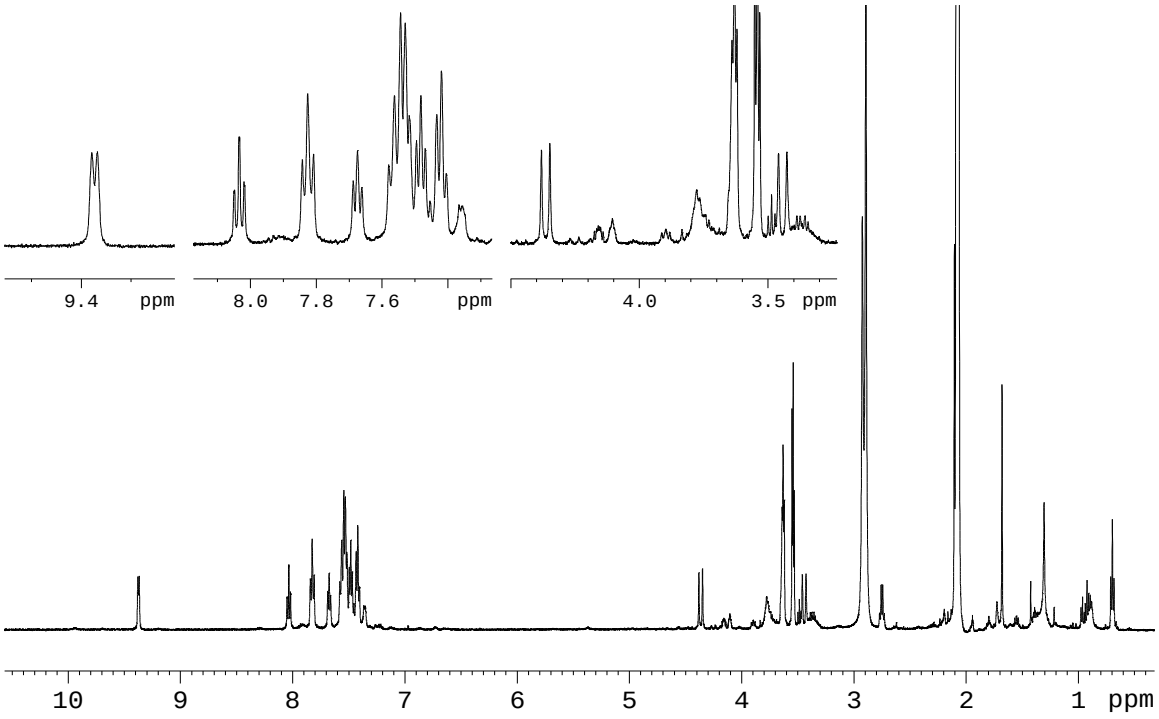
9.4 ppm
8.0 7.8 7.6 ppm
4.0 3.5 ppm
10 9 8 7 6 5 4 3 2 1 ppm

b)

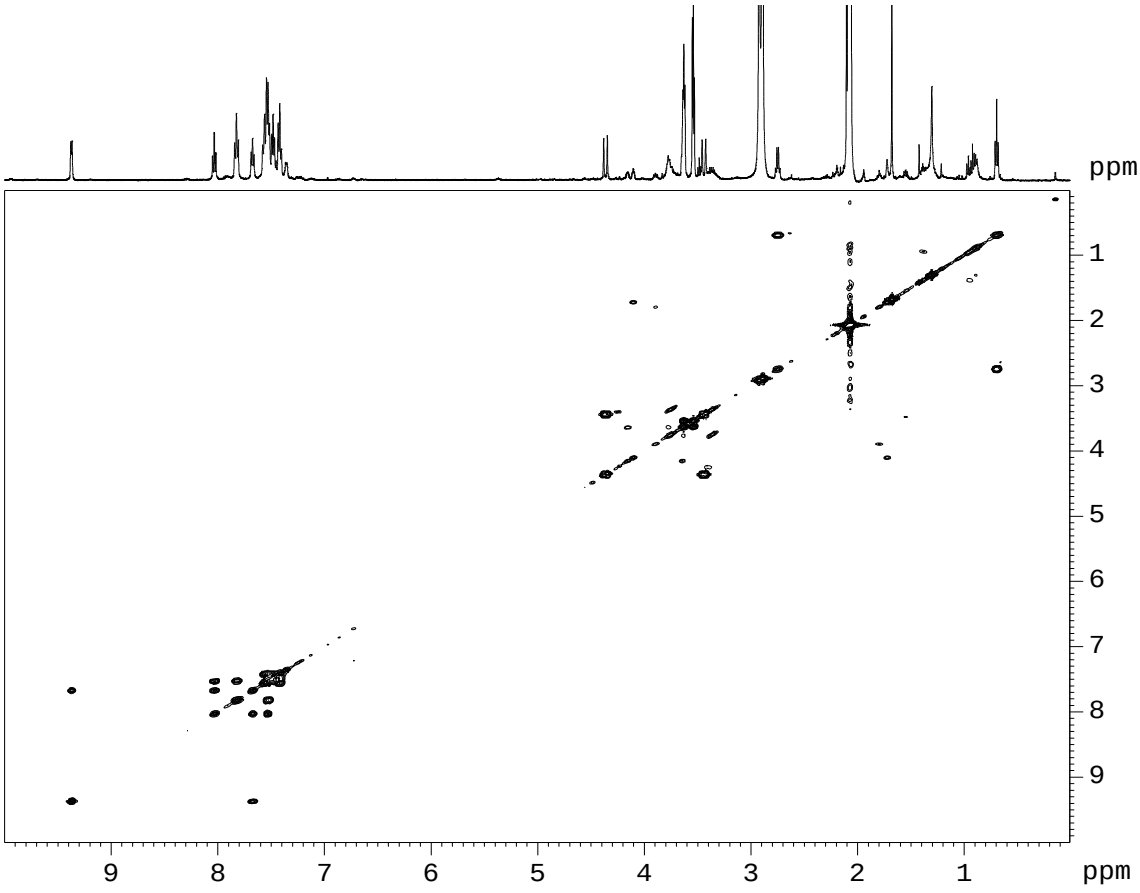
ppm
1 2 3 4 5 6 7 8 9
9 8 7 6 5 4 3 2 1 ppm

c)

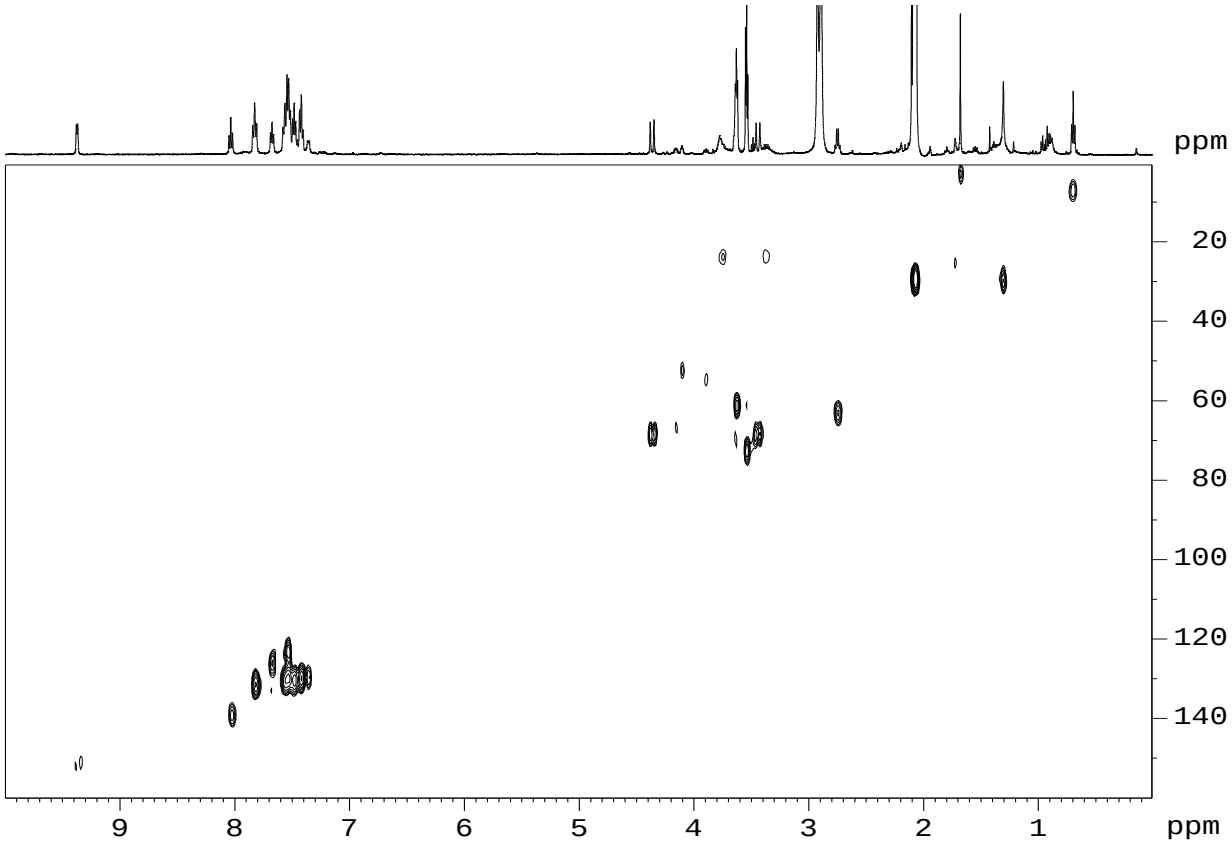
ppm
20
40
60
80
100
120
140
9
8
7
6
5
4
3
2
1
ppm

d)

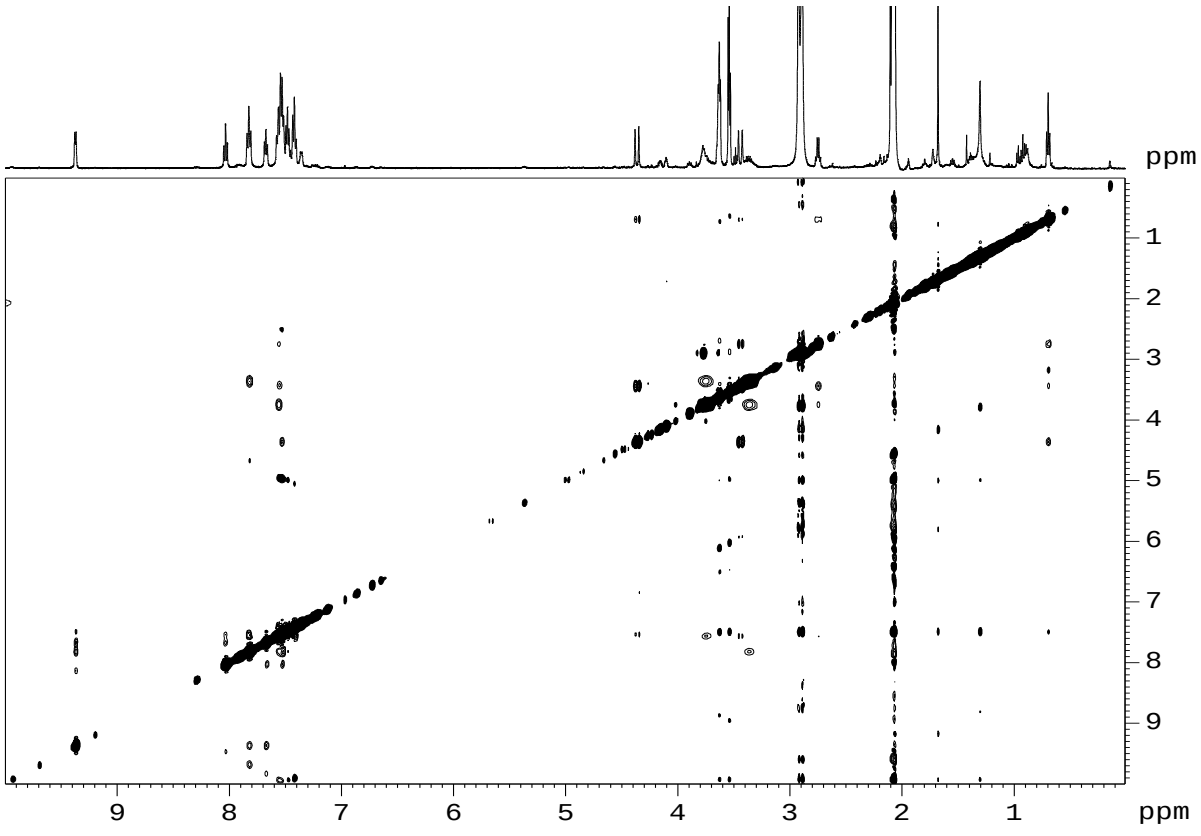
ppm
1
2
3
4
5
6
7
8
9
9
8
7
6
5
4
3
2
1
ppm

e)

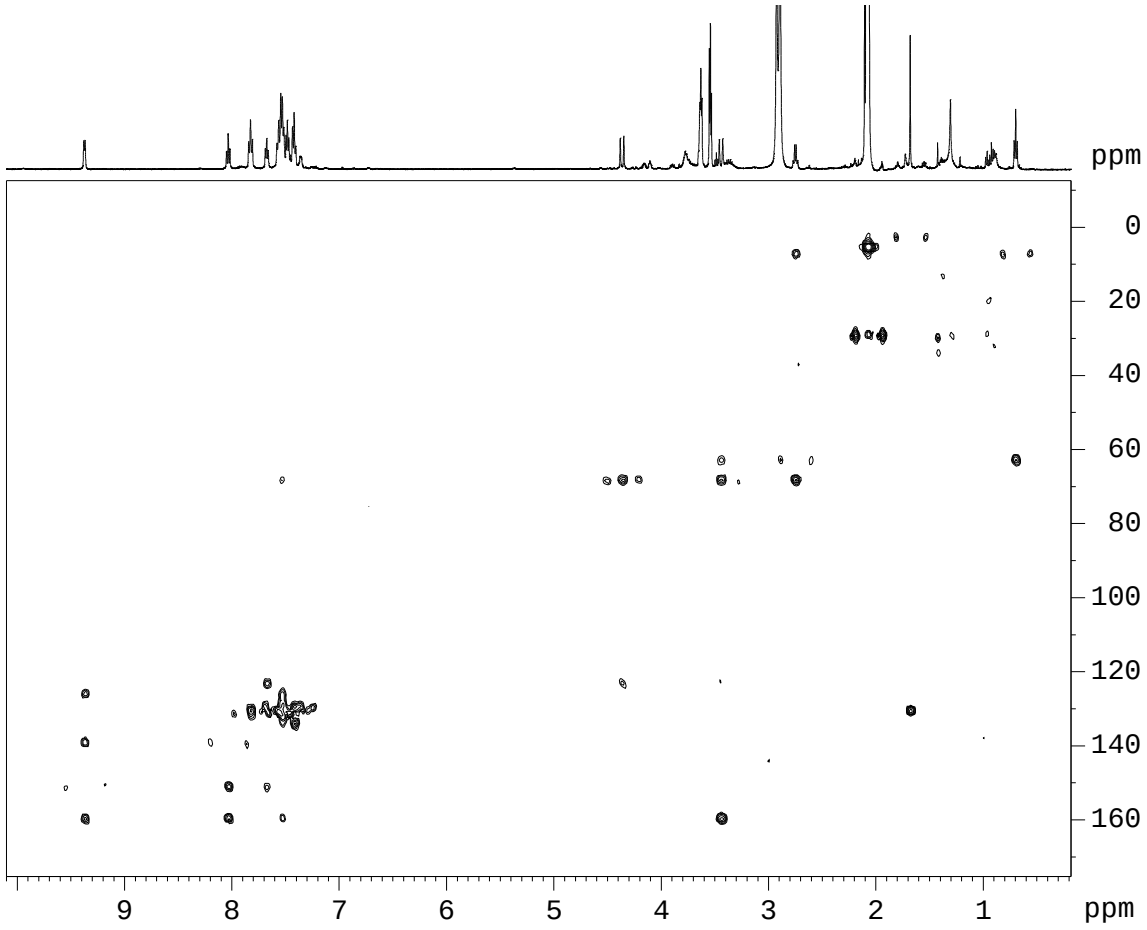
ppm
0
20
40
60
80
100
120
140
160
9
8
7
6
5
4
3
2
1
ppm

f)

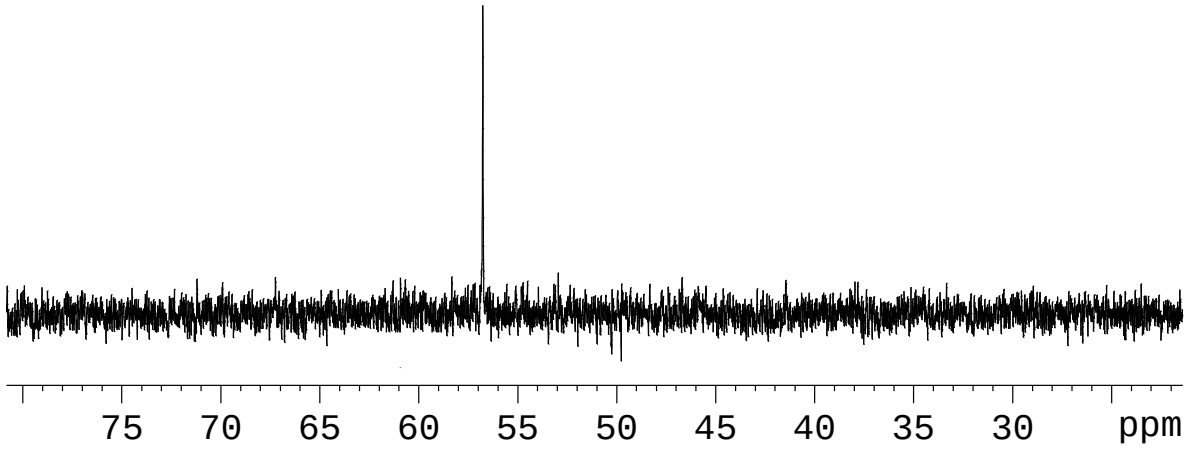
75
70
65
60
55
50
45
40
35
30
ppm

Figure S3

a)

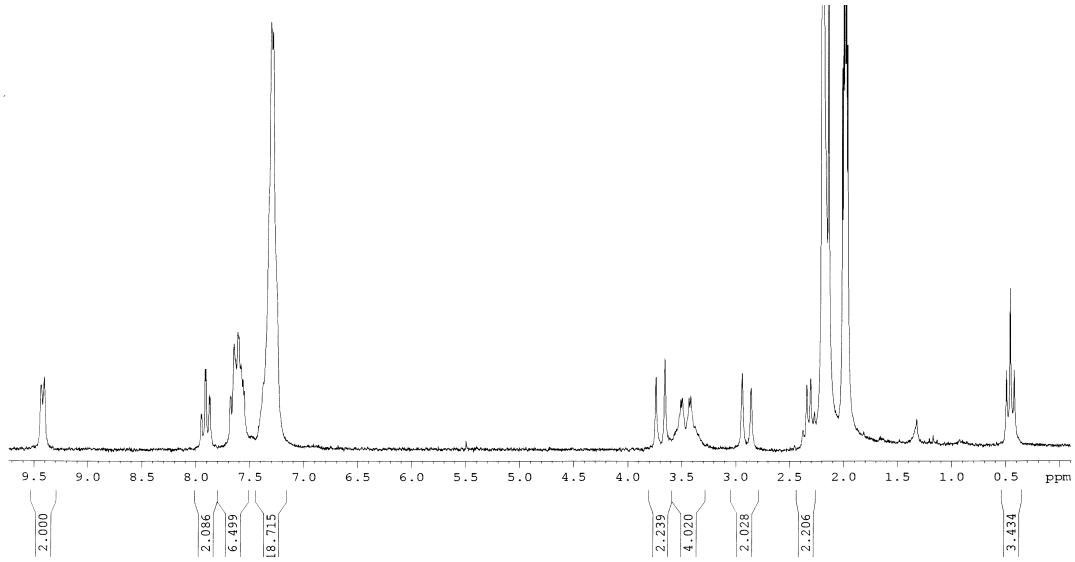
9.5
9.0
8.5
8.0
7.5
7.0
6.5
6.0
5.5
5.0
4.5
4.0
3.5
3.0
2.5
2.0
1.5
1.0
0.5
ppm
2.000
2.086
6.499
18.715
2.239
4.020
2.028
2.206
3.434

Figure S4

a)

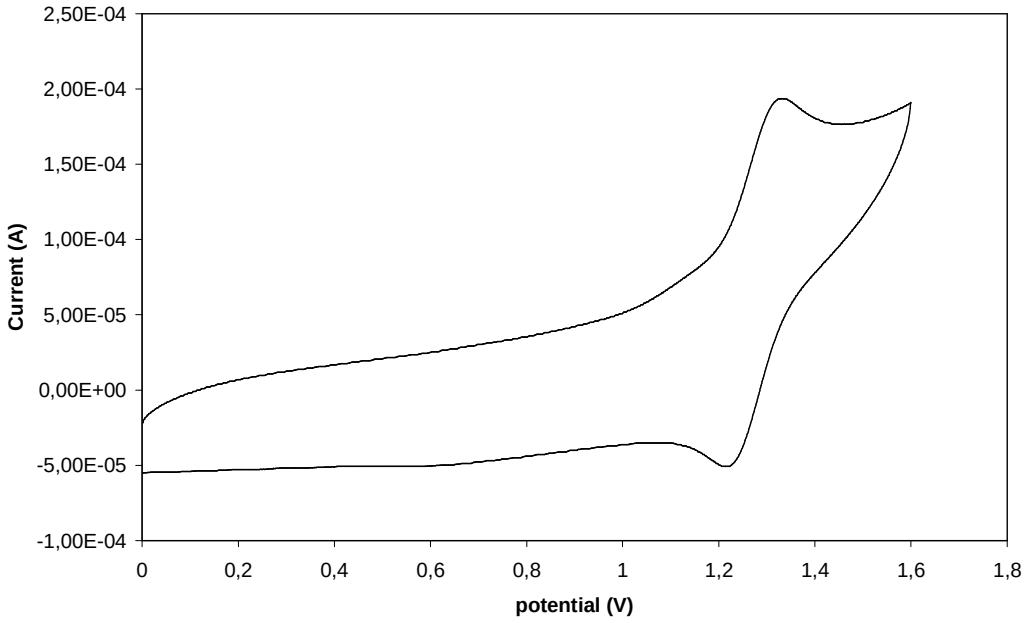
2,50E-04
2,00E-04
1,50E-04
1,00E-04
5,00E-05
0,00E+00
-5,00E-05
-1,00E-04
Current (A)
0
0,2
0,4
0,6
0,8
1
1,2
1,4
1,6
1,8
potential (V)

b)

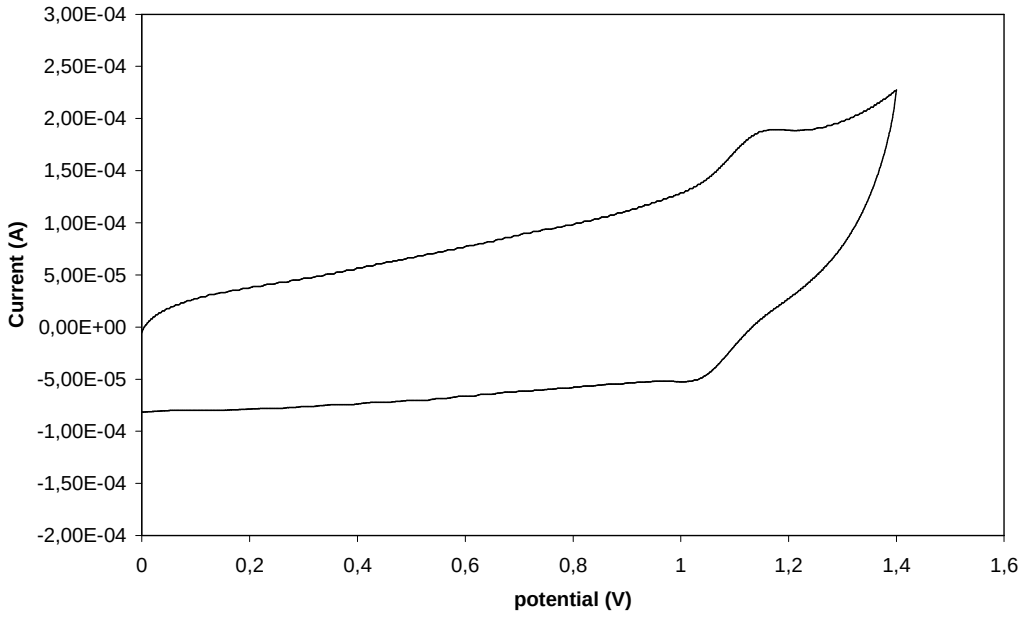
3,00E-04
2,50E-04
2,00E-04
1,50E-04
1,00E-04
5,00E-05
0,00E+00
-5,00E-05
-1,00E-04
-1,50E-04
-2,00E-04
Current (A)
0
0,2
0,4
0,6
0,8
1
1,2
1,4
1,6
potential (V)

c)

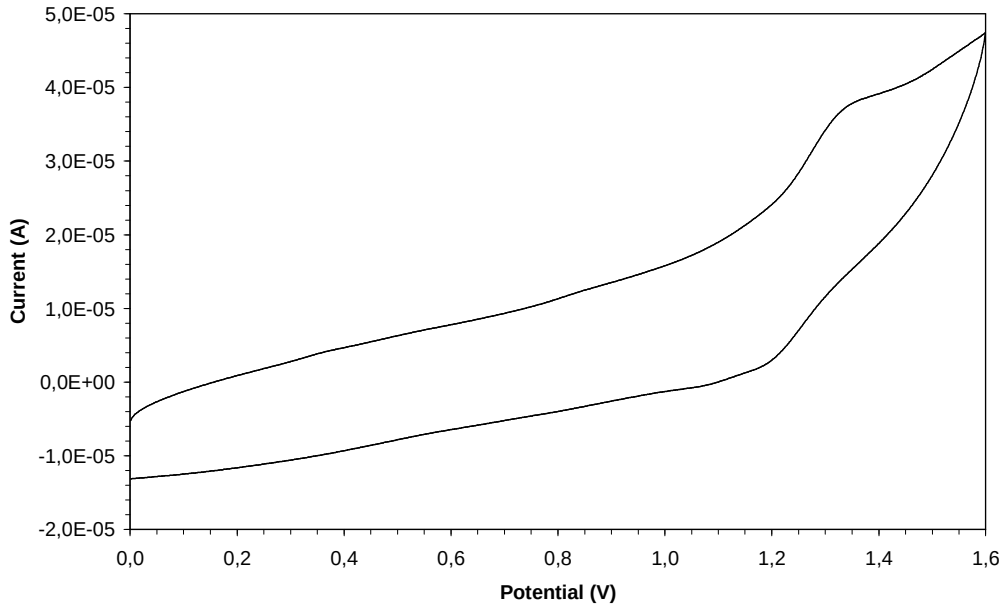
5,0E-05
4,0E-05
3,0E-05
2,0E-05
1,0E-05
0,0E+00
-1,0E-05
-2,0E-05
Current (A)
0,0
0,2
0,4
0,6
0,8
1,0
1,2
1,4
1,6
Potential (V)

Figure S5

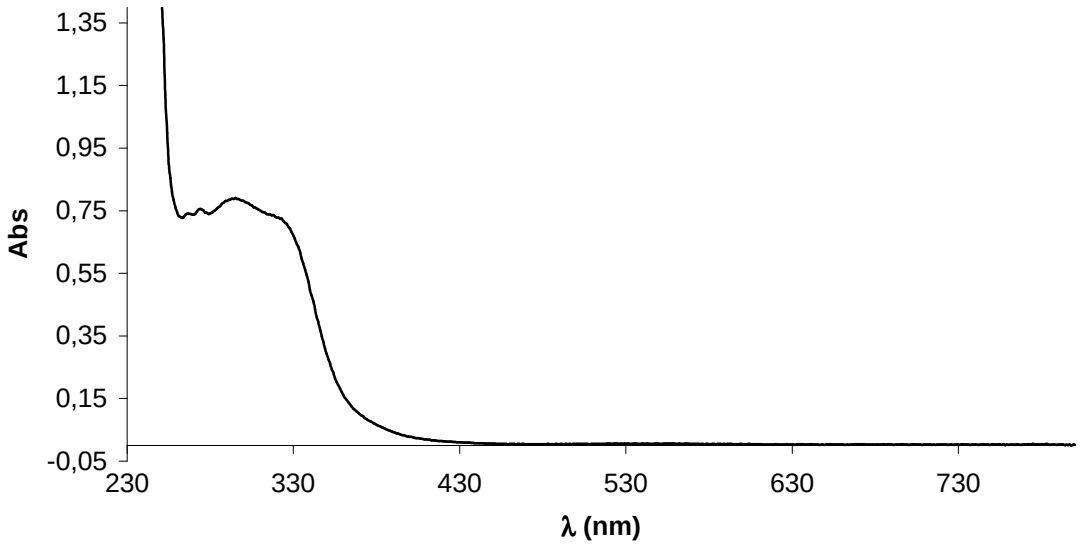

Figure S6

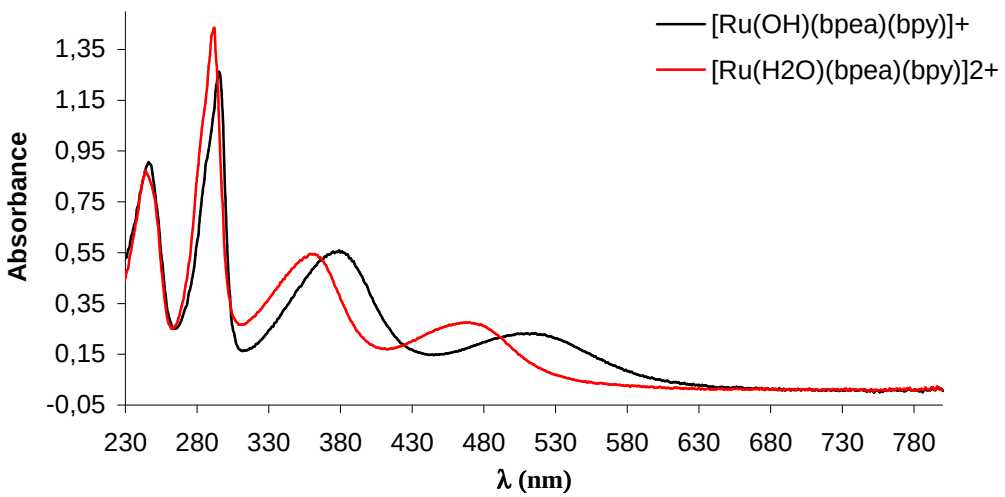
[Ru(OH)(bpea)(bpy)]+
[Ru(H2O)(bpea)(bpy)]2+
Absorbance
1,35
1,15
0,95
0,75
0,55
0,35
0,15
-0,05
230
280
330
380
430
480
530
580
630
680
730
780
λ (nm)

Figure S7

a)

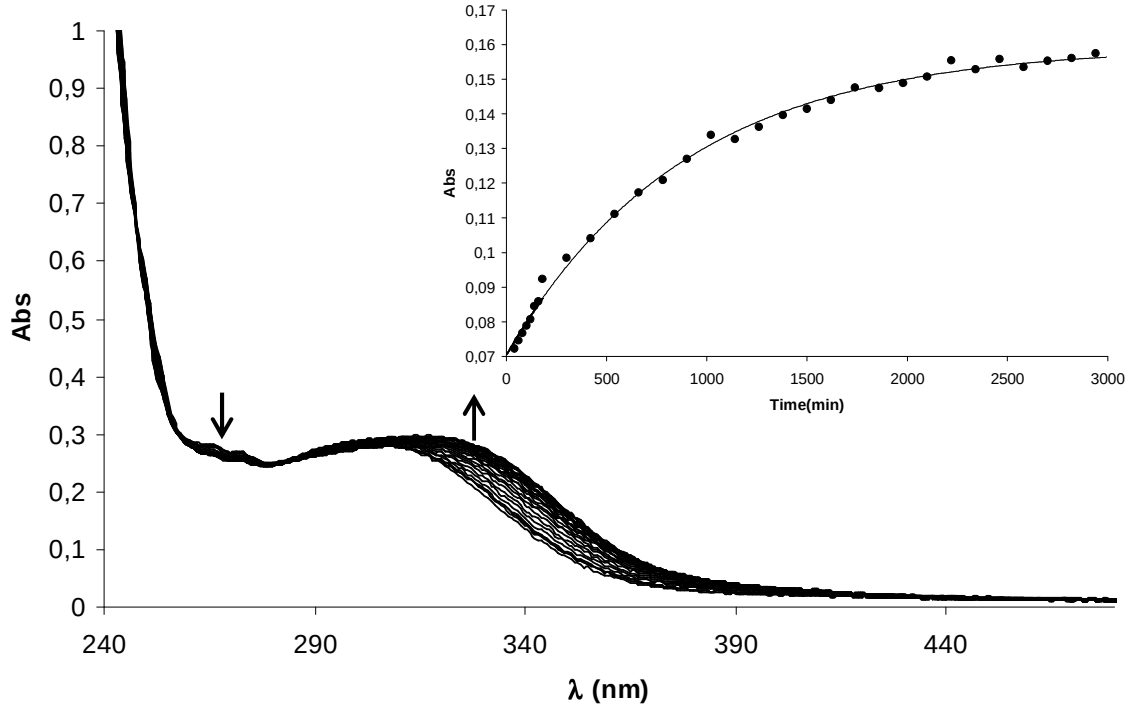

b)

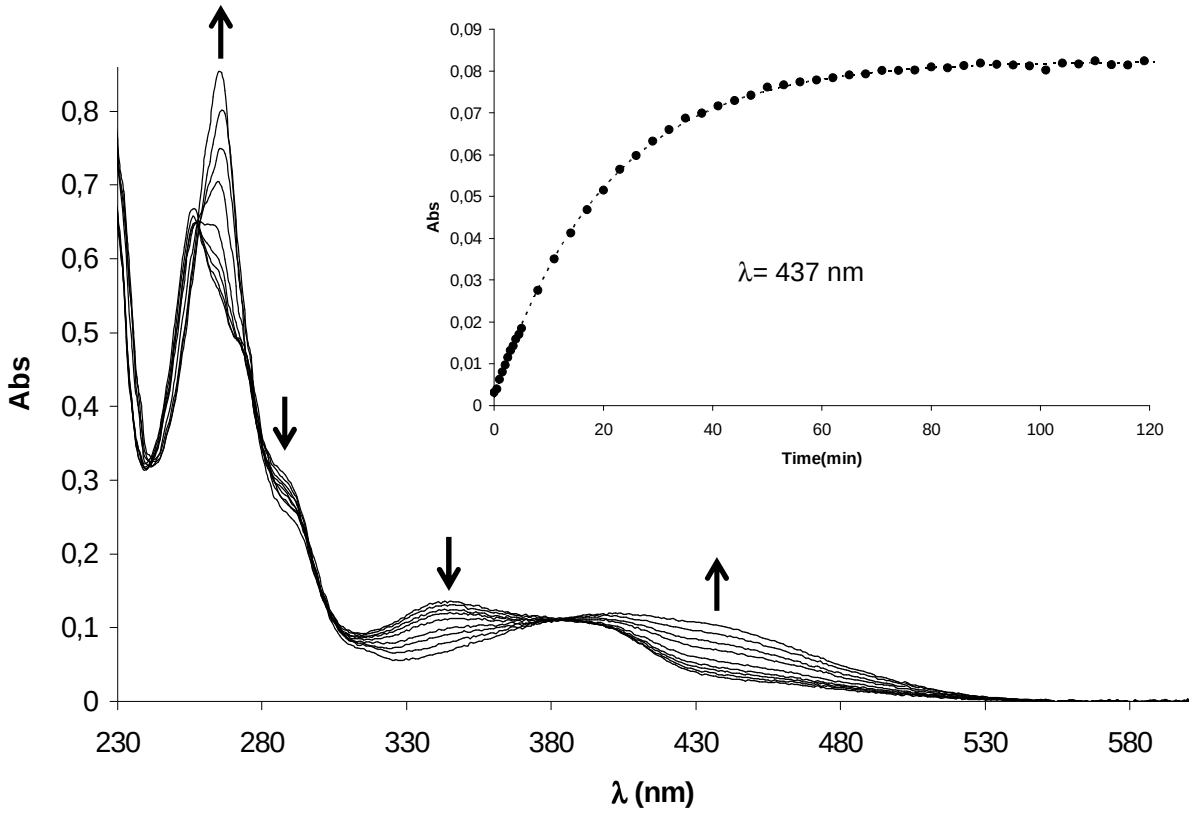

Figure S8

a)

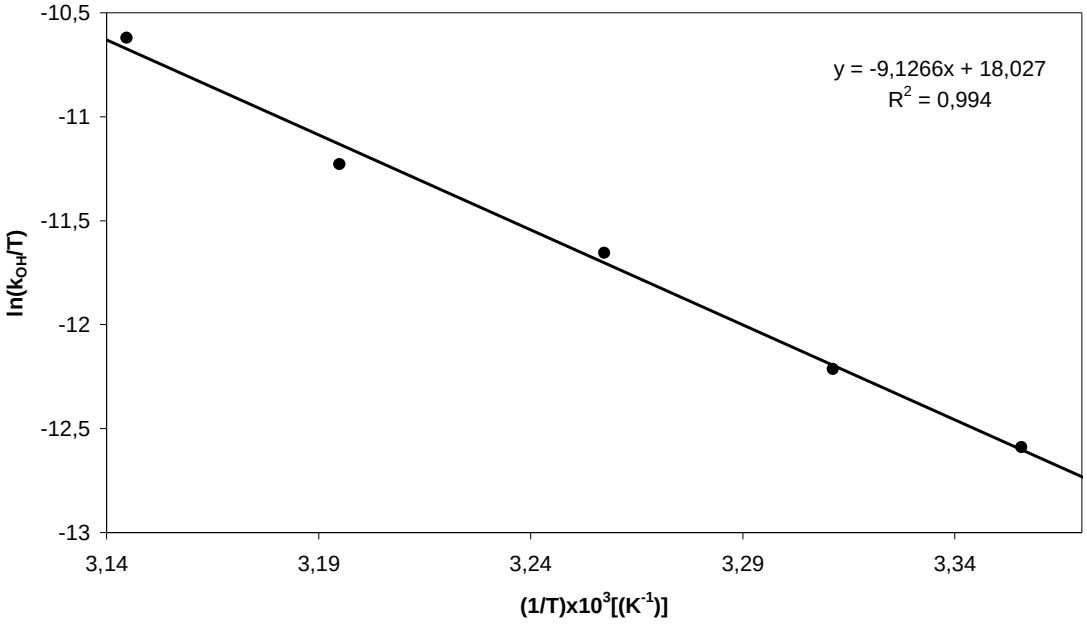
y = -9,1266x + 18,027
R2 = 0,994
-10,5
-11
-11,5
-12
-12,5
-13
3,14
3,19
3,24
3,29
3,34
ln(kOH/T)
(1/T)x10^3[(K^-1)]

b)

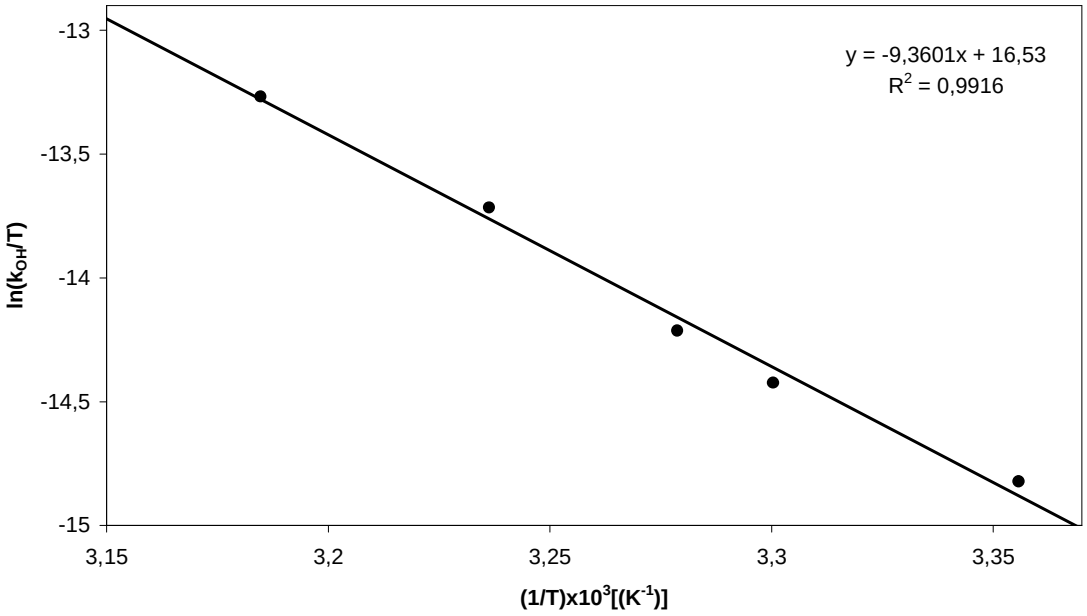
y = -9,3601x + 16,53
R2 = 0,9916
-13
-13,5
-14
-14,5
-15
3,15
3,2
3,25
3,3
3,35
ln(kOH/T)
(1/T)x10^3[(K^-1)]

c)

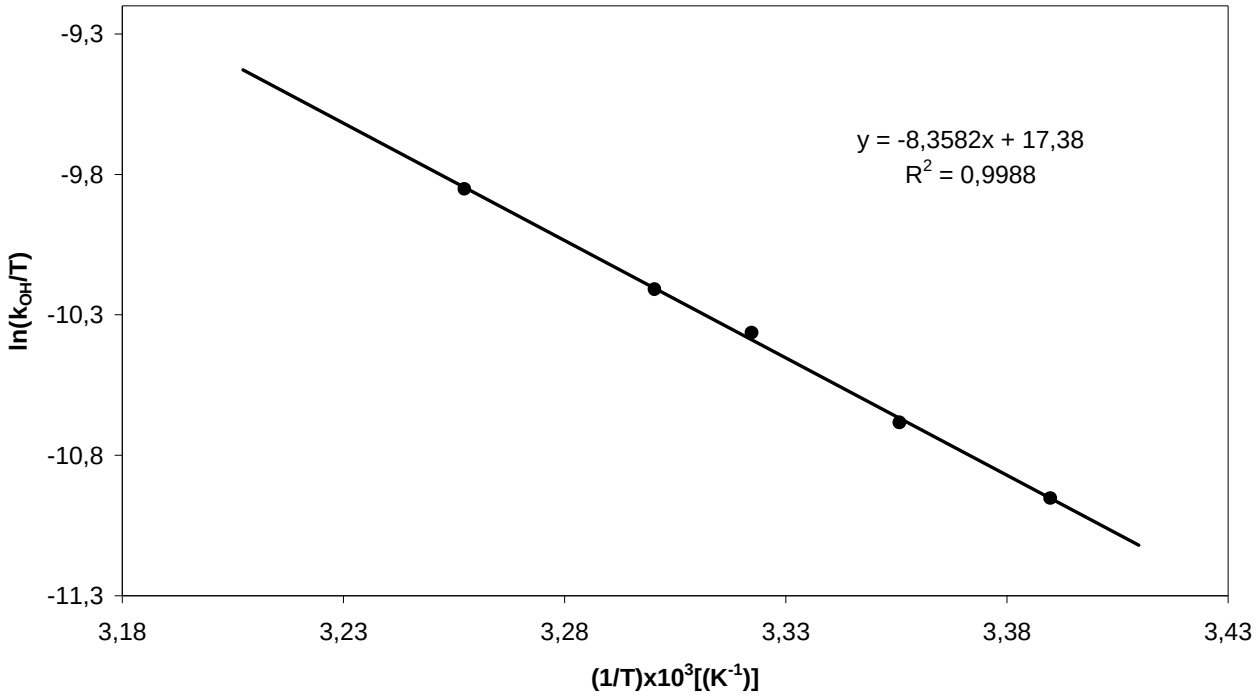
-9,3
-9,8
-10,3
-10,8
-11,3
ln(kOH/T)
y = -8,3582x + 17,38
R2 = 0,9988
3,18
3,23
3,28
3,33
3,38
3,43
(1/T)x10^3[(K^-1)]

Figure S9.

a)

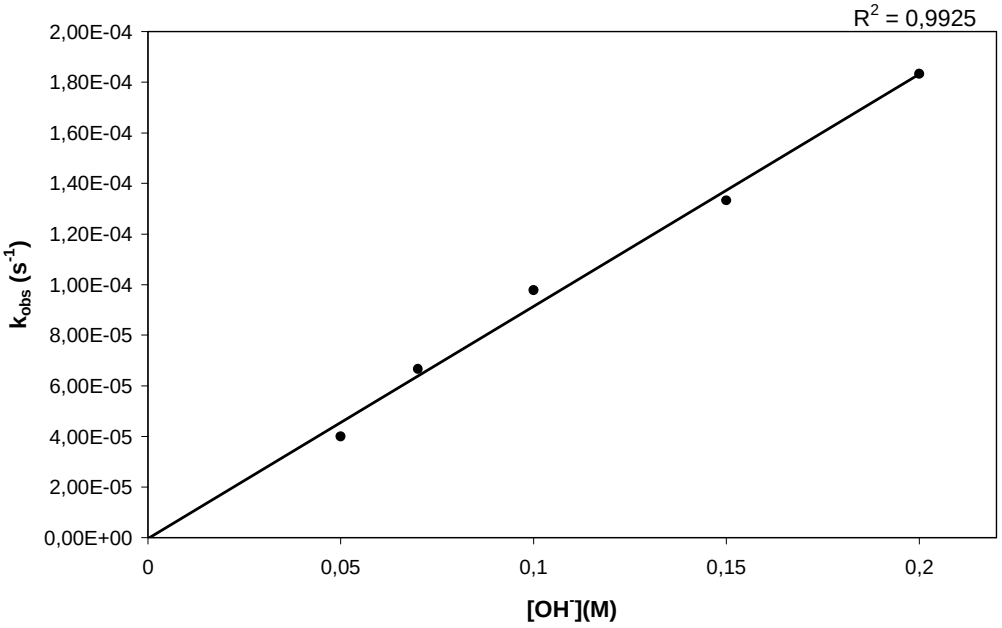
R2 = 0,9925
2,00E-04
1,80E-04
1,60E-04
1,40E-04
1,20E-04
1,00E-04
8,00E-05
6,00E-05
4,00E-05
2,00E-05
0,00E+00
kobs (s-1)
0
0,05
0,1
0,15
0,2
[OH-](M)

b)

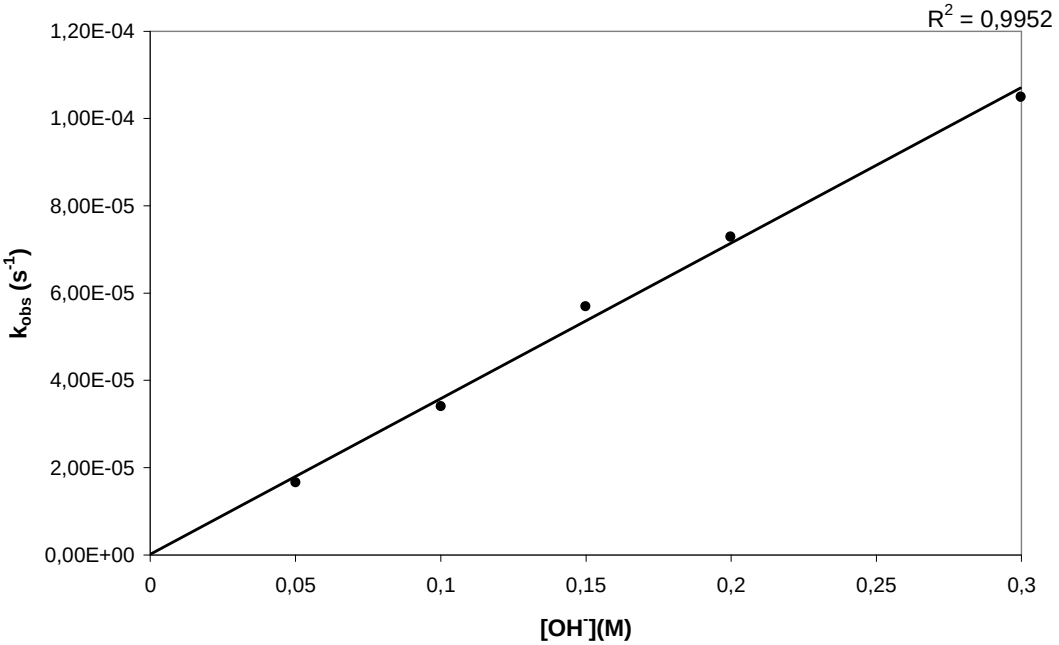
R2 = 0,9952
1,20E-04
1,00E-04
8,00E-05
6,00E-05
4,00E-05
2,00E-05
0,00E+00
kobs (s-1)
0
0,05
0,1
0,15
0,2
0,25
0,3
[OH-](M)

Figure S10

a)

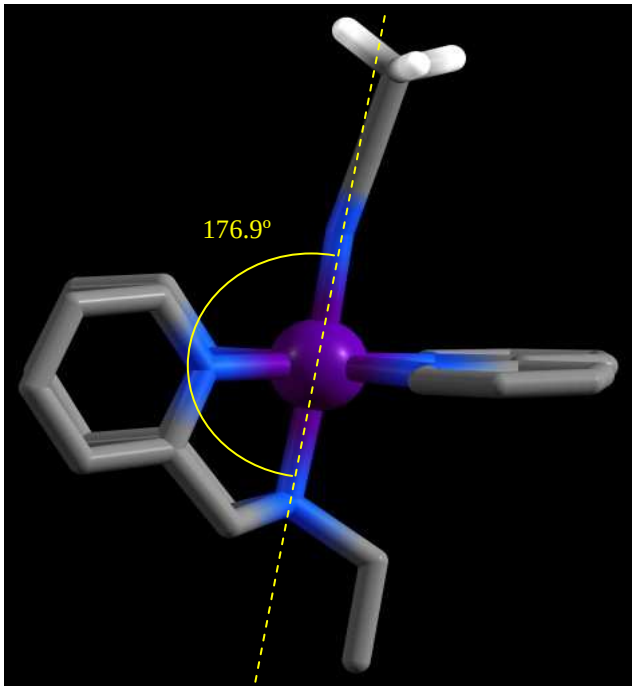

b)

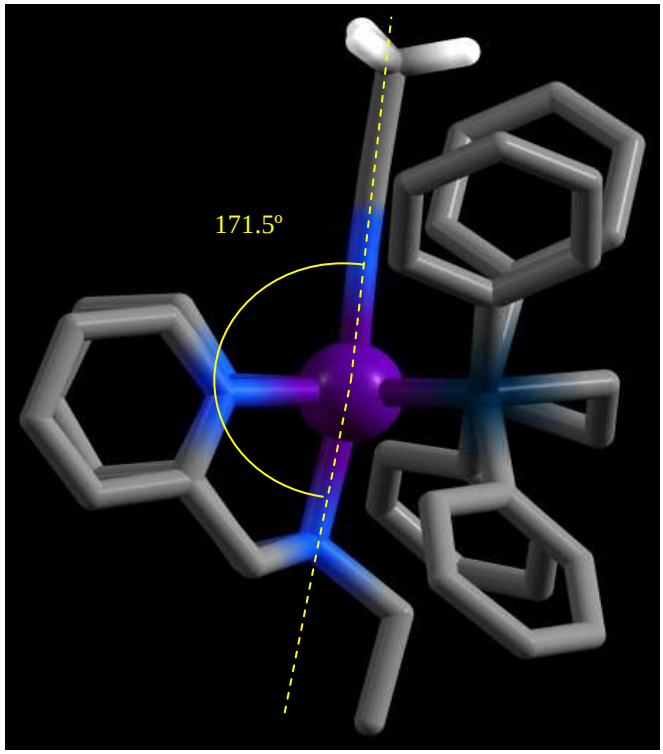

c)